

## Impact response of aluminum foam core sandwich structures

Kapil Mohan<sup>a</sup>, Tick Hon Yip<sup>a</sup>, Sridhar Idapalapati<sup>b</sup>, Zhong Chen<sup>a,\*</sup>

<sup>a</sup> School of Materials Science and Engineering, Nanyang Technological University, 50 Nanyang Avenue, Singapore 639798, Singapore

<sup>b</sup> School of Mechanical and Aerospace Engineering, Nanyang Technological University, 50 Nanyang Avenue, Singapore 639798, Singapore

### ARTICLE INFO

#### Article history:

Received 17 April 2011

Received in revised form 28 June 2011

Accepted 31 August 2011

Available online 8 September 2011

#### Keywords:

Aluminum (Al) foam

Impact

Energy absorption

Face sheets

Failure mode

### ABSTRACT

Sandwich panels, comprised of metallic foam core and face sheets, are widely used to withstand impact and blast loadings. Based on the actual application requirements, the performance can be optimized with the proper combination of face sheets design. In this paper the impact responses of aluminum foams with various tailored face sheets, whose behavior represents elastic, elastic-ideally plastic and elastic-plastic strain work hardening, were investigated experimentally. The experiment was carried out using hemispherical indenters on blocks of aluminum foam with and without the face sheet. Competing failure modes for the initiation of failure are discussed based on comparison of energy absorption capacity. Results show that increase in thickness of foam and the use of face sheet enhances the impact energy absorption capacity. The type of face sheet not only affects the energy absorption capacity but also the failure mode for the foam blocks. Aluminum foam blocks with stainless steel sheet are strong enough to withstand the pre-designated impact loading without penetration damage. At the same time, this study also provides a comparison of the impact performance, in terms of impact energy and failure mode, among blocks with different face sheets under the low velocity impact.

© 2011 Elsevier B.V. All rights reserved.

### 1. Introduction

Many metals and alloys can be foamed to achieve required relative density using various manufacturing processes [1]. During these processes, either open or closed cellular structures can be achieved. Lot of research work have been dedicated to Al metal-based alloy foams due to their good combination of properties such as high specific stiffness and strength, excellent plastic energy absorbing capabilities, good corrosion resistance, being recyclable and can be produced to near isotropic and homogeneous cellular structures [2,3]. Different types of Al foams were investigated under dynamic compression by various researchers to understand the strain rate sensitivity on various parameters such as yield stress and modulus [4–6] to use its high energy absorbing capabilities for practical applications. Most studies indicate that the strain rate sensitivity of Al foams depend upon the type of Al foam [7]. Absorption of impact energy at a low velocity of 3.7 m/s and high velocities ranging between 22 and 30 m/s was investigated by Ramachandra et al. [8] for Alporas<sup>®</sup> foam using flat ended and spherical impactors.

Performance of Al foams can be enhanced by using it as core material in a sandwich, with strong and stiff face sheets. These structures can be used in various applications including automo-

bile, aerospace, and building structures for both military and civil uses. Banhart and Seeliger [9] developed a manufacturing method for producing sandwich panel consisting of a highly porous Al foam core and Al alloy face sheets by roll-bonding Al alloy sheets to a densified mixture of metal powders and foaming agent. Other than that, traditional ways are also used to make those sandwiches, e.g. adhesive bonding. There has been intensive interest in the investigation of the performance of sandwich structures with foams under various impact loading conditions, such as bullet/blast impact for protective structures, collision in automobile structures, debris impact in aerospace structures, etc.

Performance of Al foam as core of sandwich using Al face sheets under low and high impact loading were investigated by various researchers [10–16] to understand the failure mechanisms and energy absorption capability. Destefanis et al. [10] found that bilayered bumpers made with open cell Al foam core with Al face sheets have outstanding capability to induce multiple shocks with a strong radial dispersion of the debris cloud. Hanssen et al. [2] and Zhu et al. [11–14] investigated the behavior of Al foam panels with Al sheets under blast loading using a ballistic pendulum and found that foam panels are good energy absorbers. Hou et al. [13] observed that dynamic perforation can significantly raise the perforation energy, and this energy has a linear relationship with the impact velocity for metallic sandwich structures with closed cell CYMAT<sup>™</sup> and Al sheets under ballistic speed loading. Various failure modes such as face yielding, core shear and indentation were observed for sandwich impact bending [15] while large inelastic

\* Corresponding author. Tel.: +65 6790 4256; fax: +65 6790 9081.  
E-mail address: [ASZChen@ntu.edu.sg](mailto:ASZChen@ntu.edu.sg) (Z. Chen).

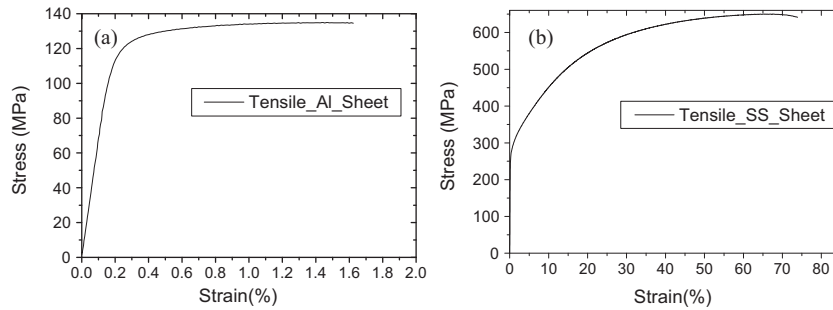


**Fig. 1.** Uniaxial stress–strain response of (a) half-hard aluminum sheet representing elastic–perfectly plastic behavior and (b) stainless steel sheet representing elastic–strain-hardening plastic behavior.

**Table 1**  
Mechanical properties of face sheets.

Sheet	Thickness (mm)	Strength (MPa)	Strain at failure
Al	0.5	134 (ultimate tensile)	17–20%*
SS	0.5	650 (ultimate tensile)	~51%*
CFRP laminate	2.0	1900 (longitudinal tensile)	1.7% (longitudinal tensile)
CFRP laminate	2.0	1050 (longitudinal compressive)	0.33% (longitudinal compressive)

\*The value was obtained from ASM Alloy Center (ASM International 2011) based the same material which possesses similar ultimate strength as the one in this work.

deformation, face wrinkle and core shear with interfacial failure were observed for these sandwich beams under dynamic loading [16].

The response of sandwich structures with Al foam core and fiber reinforced composite skins was investigated under low and high velocity impact loading using an instrumented dropping weight impact tower and using a nitrogen gas gun by Villanueva et al. and Reyes et al. [17,18]. A breakdown of the energy dissipation revealed that composite reinforced Al foam sandwich structures absorb much of the impact energy due to the bending and contact effects under high velocity impact. Various energy absorbing mechanisms such as localized indentation in the foam, fiber matrix delamination or longitudinal splitting and fiber fracture of the composite skin were observed under high velocity impact.

Mutli-layered sandwiches with foam core and various face sheets were also investigated by researchers. Mamalis et al. [19] presented a new approach on hybrid sandwich structure by combining thin metallic skins, low-density PVC foams and intermediate layers of composite/plywood to improve impact and bonding behavior. Gama et al. [20] found armor with closed cell Al foam and different skins (including composite, ceramics and rubber) perform better than armor without foam under ballistic loading. A comparative study of the mechanical behavior under bird strike impact tests by Reglero et al. [21] showed a much better performance of the aeronautical leading edge structures filled with Al foams than the empty ones (hollow structure).

It is expected that the impact performance of sandwich structures consisting of Al foam core will be different with different

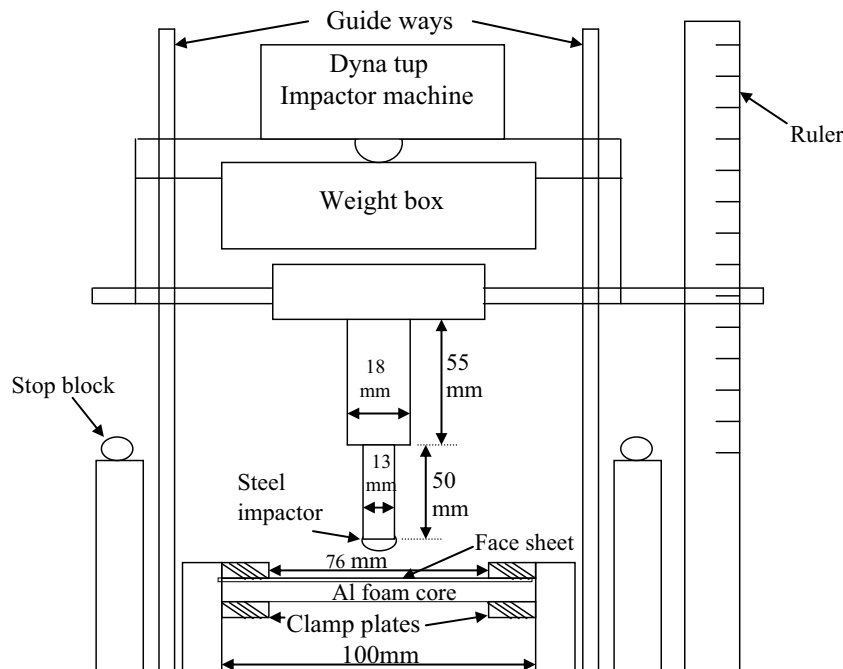


**Fig. 2.** A schematic view of the Dynatup 8250 Instron testing machine with cross-sectional view of the clamped block specimen.

face sheets due to the different mechanical behavior of the sheet materials. The selection of face sheet in metal foam cored sandwich construction depends upon the required performance of those sandwiches such as impact resistance relative to their specific weight for the best use in these applications. A systematic understanding of comparative performance of metal foam cored blocks with various face sheets under low velocity impact is still lacking. In the present work, impact studies were carried out on an aluminum alloy foam (Alporas<sup>®</sup>) blocks bonded to different type of face sheets under an impact velocity of 6.7 m/s with hemispherical tool steel punch. This impact velocity was chosen based on the guidelines for assessing the damage in roll over crash in head-on impact of automobiles [22]. The current study will evaluate the usage of such sandwiches in conforming to the safety standards for automobile parts. Meanwhile, it also provides a good comparison of the performance for sandwich structures with different face sheets under low velocity impact. The findings in terms of failure modes and load–deflection response will be compared with quasi-static indentation loading [23–26] to enable a better understanding of the usage of such sandwich structures under impact loading conditions. Face sheet materials representing elastic, elastic–perfectly plastic, and elastic–plastic work hardening behavior are chosen. In the following, the materials and the experimental procedures adopted are first described. The impact response along with energy absorption capabilities will then be discussed.

## 2. Experiment

### 2.1. Materials and properties

#### 2.1.1. Foam core

Alporas<sup>®</sup> closed cell Al foam with an average relative density of 9.5% was used as the core material for the sandwich structures as it is reported to be highly isotropic and homogeneous cellular structure [3]. The average cell size was 3.5 mm. Uniaxial tensile, compression and double-lap shear tests were conducted on the foam specimens using an Instron Universal Testing Machine 5567 under displacement control at a crosshead speed of 0.1 mm/min. Tensile strength, compressive strength and shear strength (for 20 mm thick foam) were found to be 1.51 MPa, 1.85 MPa and 1.01 MPa respectively [23].

#### 2.1.2. Face sheets

Three types of face sheets were considered in this study: purely elastic (carbon fiber reinforced polymer composite, or CFRP), elastic–perfectly plastic (aluminum alloy 1100) and elastic–plastic strain hardening (stainless steel 314). Tensile properties of the aluminum (Al) alloy and stainless steel (SS) sheets were measured by uniaxial tensile tests according to ASTM standard E8-04. The Al alloy was found to have elastic–perfectly plastic response as shown in Fig. 1(a), while stainless steel shows strain hardening behavior as shown in Fig. 1(b). CFRP composite laminates were made from unidirectional carbon fibers prepregs (supplied by Hexel Composites, Australia, 0.125 mm thickness) impregnated with epoxy matrix by hand lay up technique. The required number of prepreg sheets were stacked together and cured at 120 °C at a nominal pressure of 0.1 MPa in a vacuum bag mold for 2 h. The mechanical property measurements were described elsewhere [24]. CFRP face sheet was found to be linear elastic till fracture. The measured properties for all the face sheets are summarized in Table 1.

### 2.2. Test specimen preparation and impact test

In the present investigation, Alporas<sup>®</sup> foam of cross-section of 100 mm × 100 mm with different thicknesses 20, 30 and 40 mm

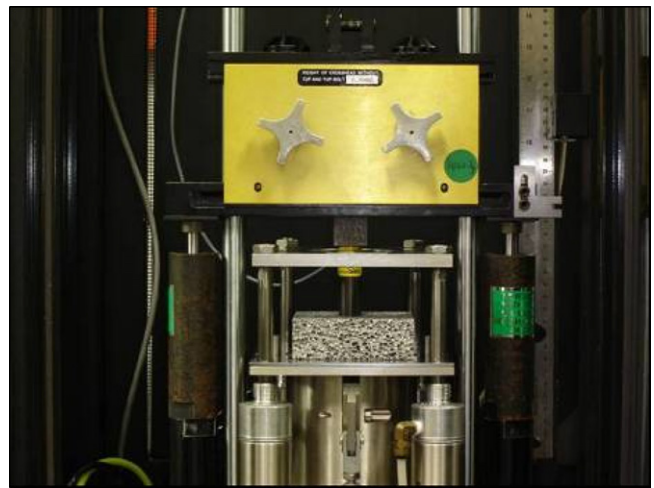


Fig. 3. Punch through of the Al foam block by impactor.

were bonded to the three types of face sheets using Redux 322 epoxy adhesive as described earlier [25].

Weight drop impact tests were carried out on foam blocks with/without face sheets using Instron DynaTup 8250 impact testing machine. These tests were carried out using a hemispherical steel tup of 13 mm diameter using rebound brake to avoid multiple impacts. A schematic diagram of Dyna Tup 8250 machine is shown in Fig. 2 with cross sectional view of the clamped specimen. Air pressure in the pneumatic pump located behind the machine was adjusted every time to keep the impact velocity at 6.7 m/s, which is much higher than the free falling speed limit of this machine. An impactor of 2.65 kg weight fell onto the specimens along two smooth guided columns through the center hole of the clamp plate of 76 mm diameter. Response of the impact test was recorded and collected from the data acquisition system in terms of load, time, energy, velocity and displacement.

Pictures of specimens after impact test were recorded and subsequently those specimens were sectioned by electron discharge machining (EDM). The damage zones were observed by a Surface Displacement Analyser (SDA). However, due to the non-conductive nature of the adhesive, EDM failed to cut the specimens at sites where the foam was crushed and adhesive was present so those sites were cut later by bench saw at low speeds. A typical picture of Al foam block of 30 mm thickness, which was punched through

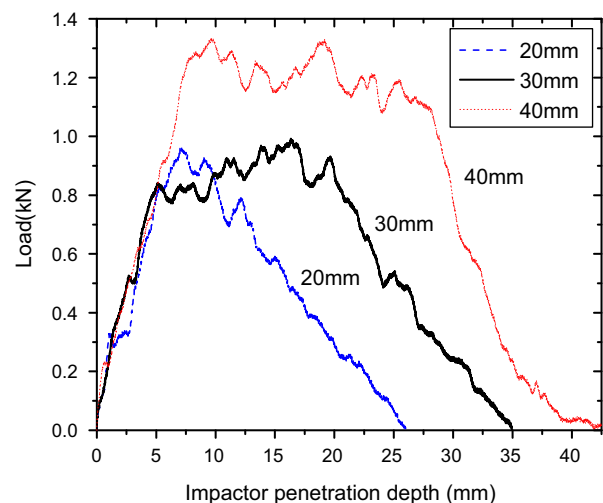
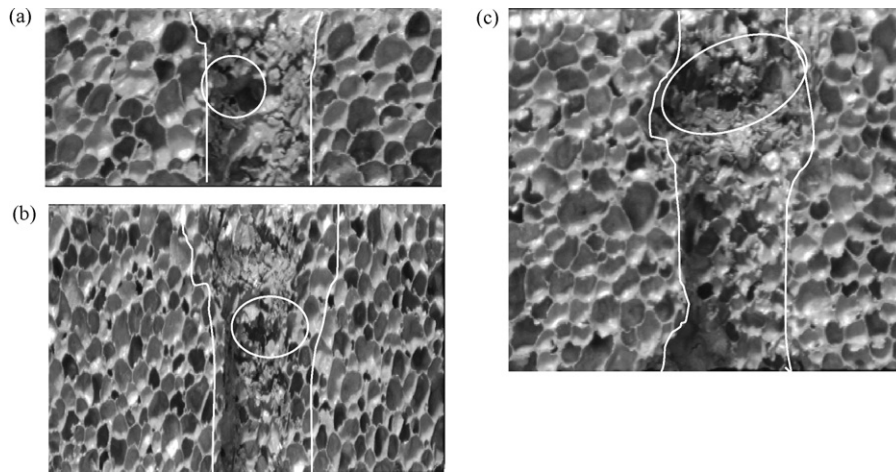


Fig. 4. Comparison of load–penetration depth behavior of foam with different thicknesses.



**Fig. 5.** Cross-sectional views of the impacted foam block with different thickness (a) 20 mm, (b) 30 mm, and (c) 40 mm. For reference of length scale, the punched holes by the steel tup diameter should be around 13 mm.

by the impactor is shown in Fig. 3. This picture further illustrates the impact loading of these blocks.

### 3. Results and discussion

#### 3.1. Impact response of foam

The load–impactor penetration depth response of Alporas<sup>®</sup> foam of different thicknesses under a weight drop impact loading is shown in Fig. 4. Impactor penetration depth is equivalent to the displacement moved by the foam block up to the stage of full penetration of the block. At the start, the load increased with displacement linearly up to an initial peak load, which represents the resistance of foam cells to penetration. This initial peak was found to be absent with spherical punch under quasi-static indentation loading [26].

Long plateau of load for around 20–25 mm displacement was observed after the initial peak load in 30 mm and 40 mm thick foam specimens, which represents the good energy absorption capacity of these foams. This long plateau in the load response was present with flat impactor but was absent with spherical impactor [8].

The response in the load–displacement curve up to the long plateau was found to be similar to the foam's response under uniaxial compressive loading [23] but the value of the load at this plateau was higher in the impact loading. This indicates that resistance to impact is derived from the crushing of cells beneath the impactor while tearing of cells at the periphery of impactor is another factor, which enhances the resistance of material. Fig. 5 of the cross-sectional view of the impacted specimens provides clear evidence for it.

The long plateau was absent for the 20 mm thick specimen, which indicates some threshold thickness of the foam whose cells

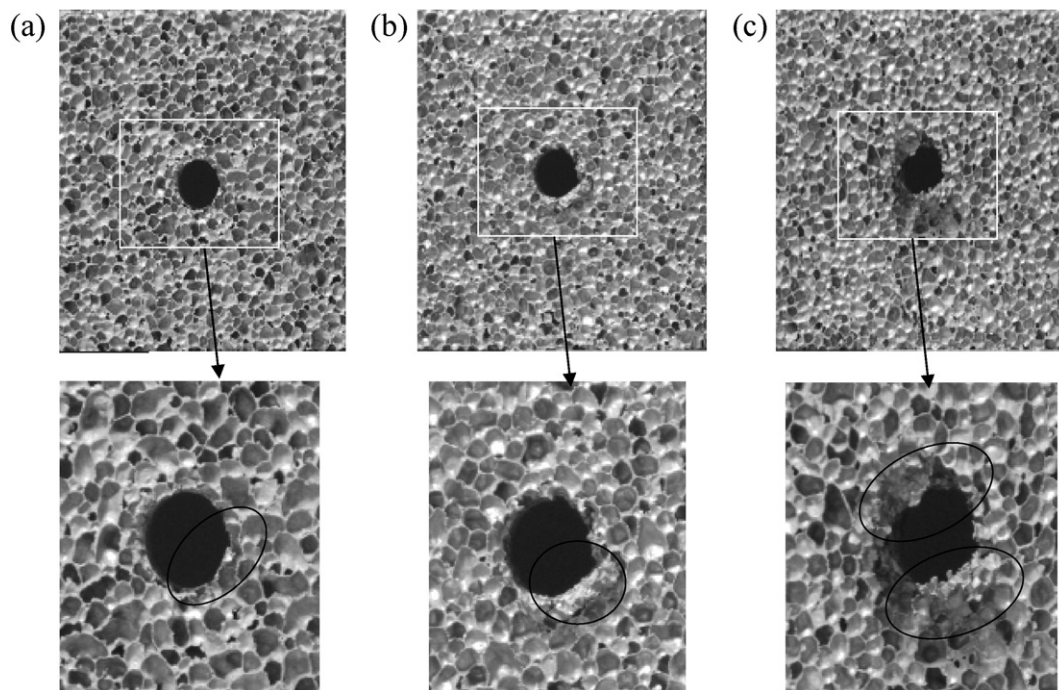


**Fig. 6.** Bottom views of the impacted specimens with no face sheets, but different foam thickness (a) 20 mm, (b) 30 mm, and (c) 40 mm. For reference of length scale, the punched holes by the steel tup diameter should be around 13 mm.

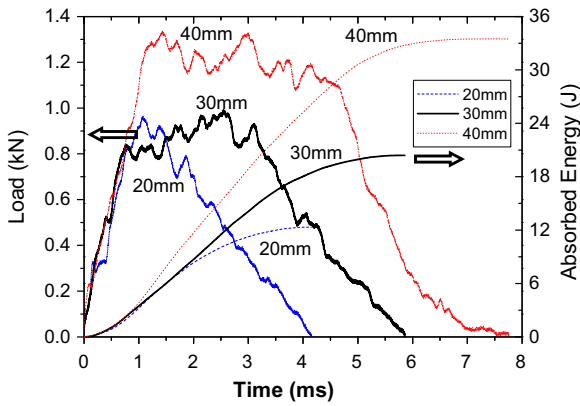


Fig. 7. Comparison of absorbed energy and load vs. time for Alporas® foam alone with various thicknesses under impact loading.

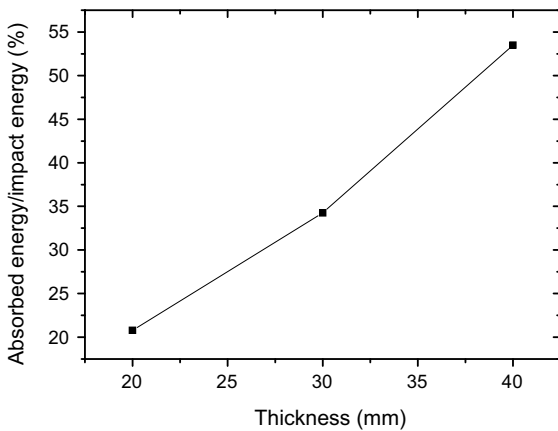


Fig. 8. Normalized absorbed energy vs. thickness of Alporas® foam under impact loading.

can provide enough resistance for penetration. The passage of impactor can be seen clearly with the two guided marked lines. The heavily damaged zones are marked by the elliptical circles in Fig. 5, which were caused by the hitting of the second cylindrical rod of the impactor (see Fig. 2).

The stiffness of all the specimens was found to be the same, which is not surprising since it is determined by the intrinsic material properties. All the specimens were punched through as shown in Fig. 6 (bottom view of the impacted specimens). This is the reason for the absence of densified zone of cells beneath the impactor,

which was present in quasi-static indentation study [26]. It is clear from Fig. 6 that as the thickness of the foam increases, the resistance increases correspondingly. This can be seen from the penetration of the foam specimen as tearing and bending occurred outside at the circumference of the hole made by the impactor.

Fig. 7 shows absorbed energy and load as a function of time of impact for the Alporas® foam with different thicknesses of 20 mm, 30 mm and 40 mm. The energy absorbing nature of these Al foams are proven by the increment in the absorbed impact energy with increased thickness. Absorbed energy was normalized with impact energy and plotted with thickness of foam as shown in Fig. 8. The trend between normalized impact energy and foam thickness was found to increase almost linearly with thickness. Extrapolating from the trend line shows that at around 69 mm thick foam block will be able to absorb 100% absorbed energy/impact energy.

### 3.2. Impact response of foam with different face sheets

The load–penetration depth response of 30 mm thick Alporas® foam with and without various face sheet of 0.5 mm in thickness under weight drop impact loading is shown in Fig. 9. Load increased almost linearly with displacement up to an initial peak for all the blocks with different face sheet under impact loading. This was accomplished by the bending and stretching of the face sheets at the periphery of the impactor as shown in Fig. 10 (cross-sectional view of the impacted specimens). Stiffness of all the specimens was different, which is a result of the different face sheet materials used.

The load initially increased linearly with displacement in the case of foam block with elastic–perfectly plastic Al alloy face sheet. There was a strong increase in the responding load due to stretching of the face sheet. After the initial peak, failure occurred due to face sheet yielding and the load decreased with the displacement. The sudden drop in the load was due to the reduction in the stiffness. The decrease in the load continued up to the point of punch through of the face sheet. After that only the foam cell resisted the penetration, which produces a similar load–displacement response with the one of foam block alone. Face sheet yielding was also found to be failure initiation mechanism for blocks with Al face sheet in the study by Yu et al. [15]. However, core shear and indentation were not observed in the present study. This could be due to the difference in the testing specimen geometry and dimension. Face sheet yielding and punching with resistance of foam cells can be seen clearly in Fig. 10(b).

In the case of stainless steel face sheets, only face sheet bending was observed and there was a strong hardening due to sheet stretching and bending. The face sheet material has to stretch to accommodate to the punch profile. The high hardening rate in the

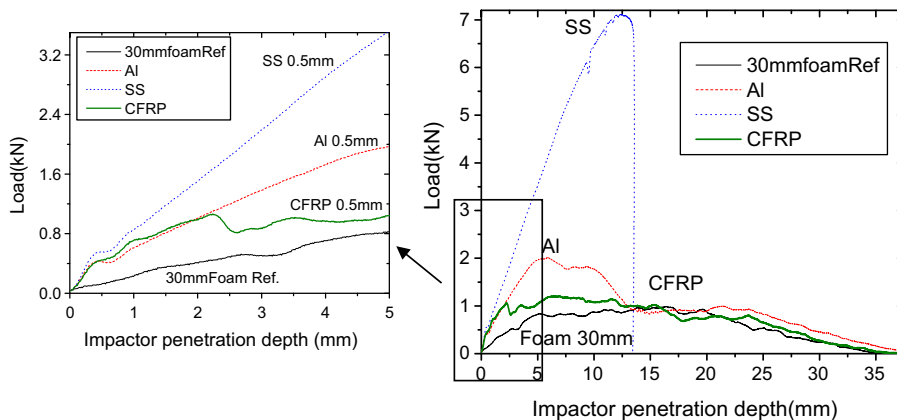
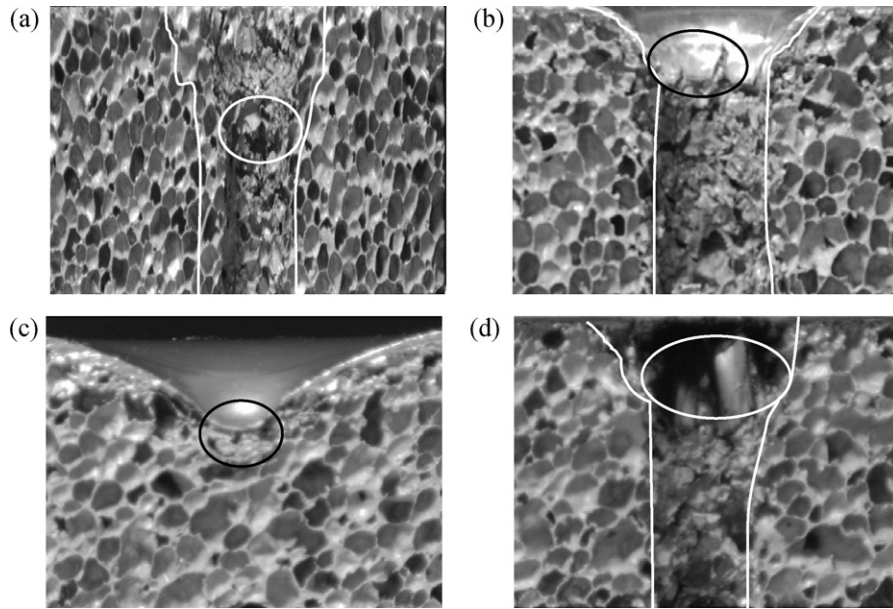


Fig. 9. Comparison of load–penetration depth behavior of foam of 30 mm thickness with different face sheets of 0.5 mm thickness under impact loading.



**Fig. 10.** Cross-sectional view of the impacted foam block with 30 mm thickness (face sheets thickness 0.5 mm) (a) without face sheet, (b) Al, and (c) SS and (d) CFRP. For reference of length scale, the punched holes by the steel tup diameter should be around 13 mm.

case of SS face sheet had a clear effect on the initial response of the sandwich structure. Further loading resulted in slight detachment of the SS sheet from the adhesive as shown at the corner of the top view of impact block in Fig. 11(c). This behavior was similar to the one when these types of specimens were tested under quasi-static indentation with spherical and flat punches [26]. As shown in Fig. 11, all the specimens were impacted through the thickness except the block with stainless steel due to its high strength.

The load–displacement response of blocks with carbon fiber reinforced plastic face sheet was found to be almost linear but were

stiffer than blocks with Al sheets because of the high stiffness of CFRP sheets. However, after a few transverse cracks appeared in the face sheet from the impact, the load decreased with displacement due to reduction in the stiffness. Beyond this, the response was similar to the foam block alone. The occurrence of these cracks is most likely due to the low transverse strength of these laminates as compared to the longitudinal strength. Face sheet punching was observed to be the final failure mechanism for this type of sample block, while face sheet bending is the initial failure mechanism, which is reflected by the bending of the face sheets as seen in the

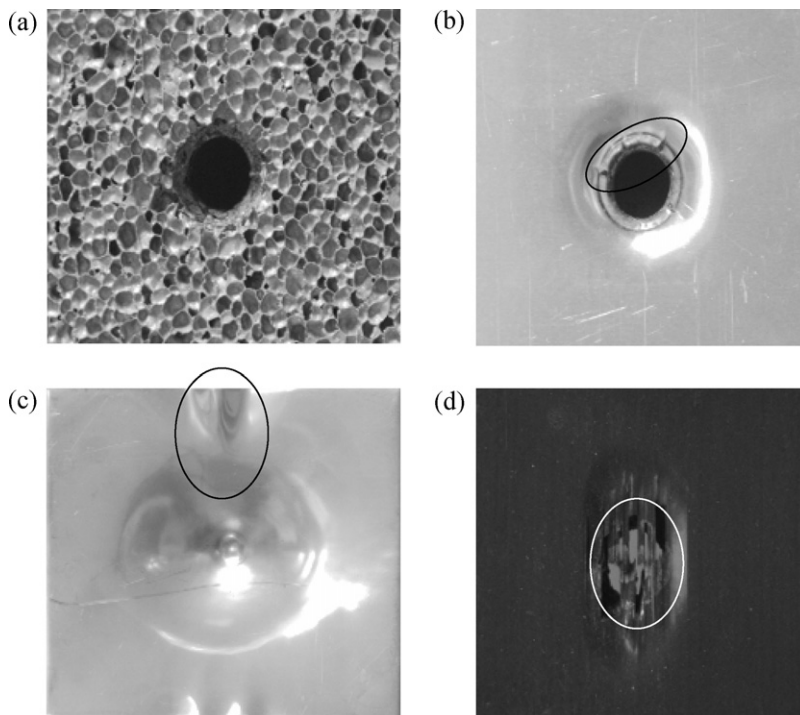


**Fig. 11.** Top views of the impacted Alporas<sup>®</sup> foam specimens (face sheets thickness 0.5 mm) (a) without face sheet, (b) Al, and (c) SS and (d) CFRP. For reference of length scale, the punched holes by the steel tup diameter should be around 13 mm.

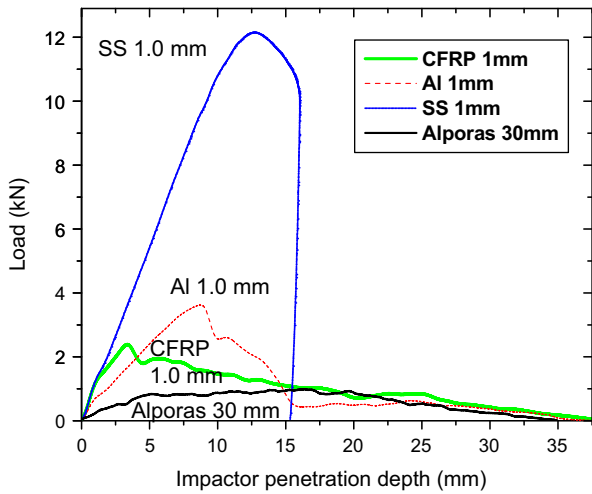


Fig. 12. Comparison of load–penetration depth behavior of foam of 30 mm thickness with different face sheets of 1.0 mm thickness under impact loading.

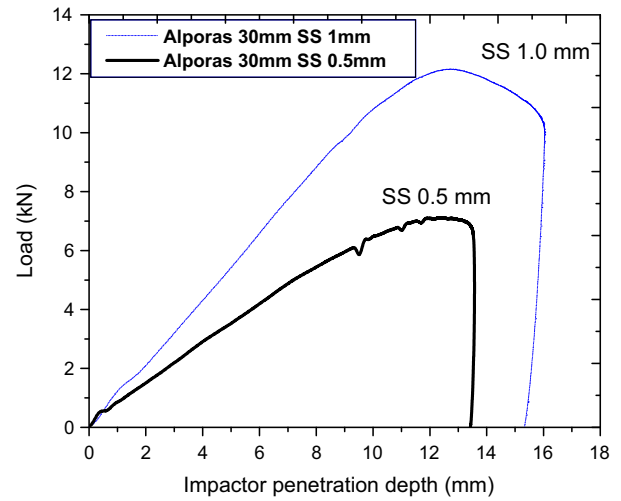


Fig. 13. Comparison of load–penetration depth behavior of foam of 30 mm thickness with SS face sheets of different thicknesses under impact loading.

top and cross-sectional views (Figs. 10(d) and 11(d)). These blocks were found to have more localized damage because of the higher strain rate compared to blocks under quasi-static indentation [26].

The load–penetration depth response of 30 mm thick Alporas® foam with and without various face sheet of 1 mm thickness under weight drop impact loading is shown in Fig. 12. The response of these Alporas® blocks were found to be similar to face sheets with 0.5 mm thickness but the amount of energy absorbed was more in blocks with 1 mm face sheets as seen in Fig. 13 for SS face sheets. It is worth mentioning that although the amount of absorbed energy was increased in blocks with the 1 mm thick face sheet but we have to take note of the weight increase due to the extra 0.5 mm SS sheet used. In other words, the beneficial effect from the face sheet thickness increase might not be extrapolated for too far.

The energy absorbed and load as a function of time of impact for Alporas® foam block with various face sheets of 0.5 mm thickness is shown in Fig. 14. The load–time response for blocks with 30 mm thick foam core and different face sheets is similar to their load–displacement responses, which indicates linear relationship exists between displacement and time.

The load–penetration depth response of 40 mm thick Alporas® foam with different face sheets under a weight drop impact loading is shown in Fig. 15. The trend was found to be similar to the blocks of 30 mm thickness, but the difference lies in the increase in the load and the decrease in the displacement traveled by the impactor in the case of the thicker foam. The more rigid behavior is due to larger amount of membrane stretching and bending effect with thicker

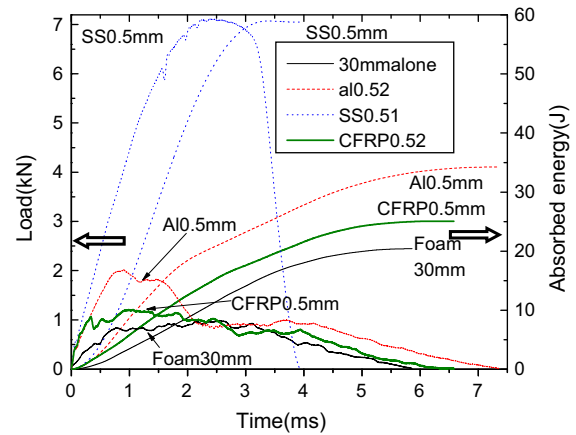


Fig. 14. Absorbed energy and load as a function of time for the impact of Alporas® foam blocks of 30 mm thickness with different face sheets.

face sheets. Top and cross-sectional views of impacted blocks were found to be similar to 30 mm thick blocks, indicating that the failure mechanisms are the same. The load–penetration depth response of Alporas® foam of 40 mm thickness with different face sheets of 1 mm thickness under a weight drop impact loading is shown in Fig. 16. It shows again similar response as the one with 0.5 mm thick face sheets.

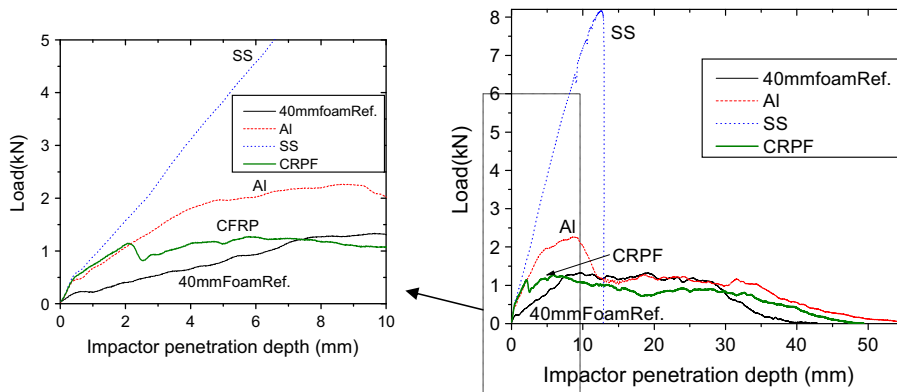
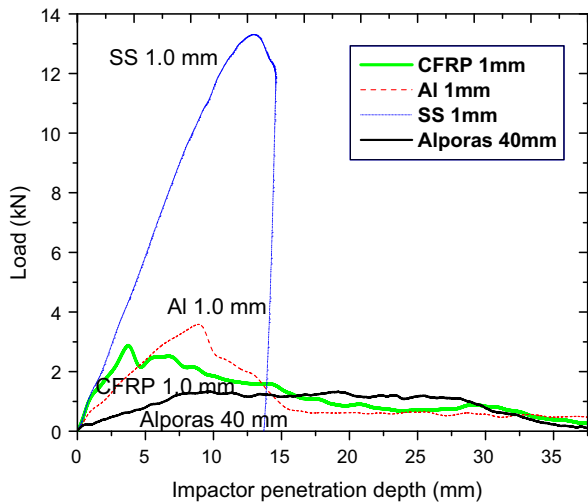
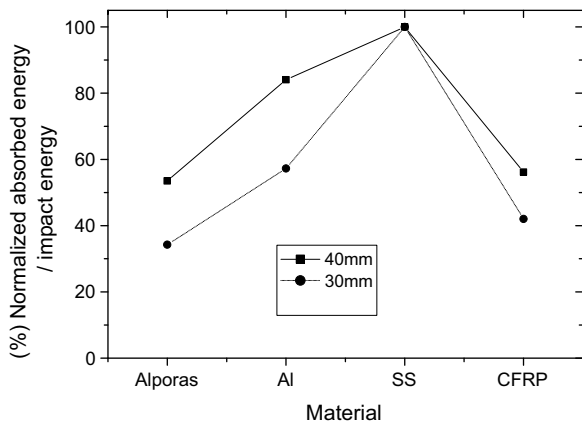


Fig. 15. Comparison of load–penetration depth behavior of foam of 40 mm thickness with different face sheets of 0.5 mm thickness under impact loading.



**Fig. 16.** Comparison of load-impactor penetration depth behavior of foam of 40 mm thickness with different face sheets of 1.0 mm thickness under impact loading.



**Fig. 17.** Normalized absorbed energy vs. blocks of Alporas® foam of 30 and 40 mm thickness with different face sheets of 0.5 mm thickness under impact loading.

Absorbed energy, normalized by the impact energy and plotted with thickness, is shown in Fig. 17 for foams core of 30 and 40 mm thick. The trend of normalized absorbed energy with impact energy was found to be similar in the 30 mm and 40 mm thick blocks but the amount of absorption is higher for the 40 mm thick blocks because of the relative higher percentage of foam cells. Almost all the impact energy was absorbed by block with SS and left an indent mark on the face sheet, this was similar to the one under spherical punch under static indentation [26].

#### 4. Conclusions

Sample blocks with aluminum foam core and various face sheets including Al, SS, and CFRP were studied under an impact

loading with a velocity of 6.7 m/s. Blocks with SS face sheet absorbed almost all the impact energy and proved to be the best choice as energy absorber in comparison with blocks with other face sheet materials. Foam core collapsing and tearing at the periphery of impactor were found as the failure mechanisms for samples without any face sheet. Face sheet yielding was found to be failure initiation mechanism for blocks with Al alloy face sheet, while face sheet bending and stretching were found to be the initiating failure mechanisms for blocks with SS and CFRP face sheets. Delamination appeared later in SS sheets during impact in this study.

Face sheet punching was found to be the only final failure mechanism observed for the foam blocks having different face sheets except SS, but the amount of energy absorption depends on the type of face sheet. Energy absorbing capacity was found to be higher for increased thickness of the foam. In summary, the current work provides general understanding of the effect of face sheet material, thickness and foam core size on the energy absorption performance as well as the failure mechanisms of a sandwiched panel under a low velocity impact loading. The performance of those sandwiches should be further evaluated in other loading conditions such as fatigue to determine their safety for practical applications.

#### References

- [1] J. Banhart, Prog. Mater. Sci. 46 (2001) 559–632.
- [2] A.G. Hanssen, L. Enstock, M. Langseth, Int. J. Impact Eng. 27 (2002) 593–618.
- [3] A.E. Simone, L.J. Gibson, Acta Mater. 46 (1998) 3109–3123.
- [4] V.S. Deshpande, N.A. Fleck, Int. J. Impact Eng. 24 (2000) 277–298.
- [5] T. Mukai, H. Kanahashi, T. Miyoshi, M. Mabuchi, T.G. Nieh, K. Higashi, Scripta Mater. 40 (1999) 921–927.
- [6] H. Kanahashi, T. Mukai, Y. Yamada, K. Shimozima, M. Mabuchi, T.G. Nieh, K. Higashi, Mater. Sci. Eng. A 280 (2000) 349–353.
- [7] J. Gassan, W. Harwick, J. Mater. Sci. Lett. 20 (2001) 1047–1048.
- [8] S. Ramachandra, P.S. Kumar, U. Ramamurthy, Scripta Mater. 49 (2003) 741–745.
- [9] J. Banhart, H.-W. Seeliger, Adv. Eng. Mater. 10 (9) (2008) 793–802.
- [10] R. Destefanis, F. Schafer, M. Lambert, M. Faraut, E. Schneider, Int. J. Impact Eng. 29 (2003) 215–226.
- [11] F. Zhu, Z. Wang, G. Lu, L. Zhao, Mater. Des. 30 (2009) 91–100.
- [12] F. Zhu, L. Zhao, G. Lu, E. Gad, Int. J. Impact Eng. 36 (2009) 687–699.
- [13] W. Hou, F. Zhu, G. Lu, D.-N. Fang, Int. J. Impact Eng. 37 (2010) 1045–1055.
- [14] F. Zhu, L. Zhao, G. Lu, Z. Wang, Adv. Struct. Eng. 11 (5) (2008) 525–536.
- [15] J. Yu, E. Wang, J. Li, Z. Zheng, Int. J. Impact Eng. 35 (2008) 885–894.
- [16] L. Jing, Z. Wang, J. Ning, L. Zhao, Composites B 42 (2011) 1–10.
- [17] G.R. Villanueva, W.J. Cantwell, Comput. Sci. Technol. 64 (2004) 35–54.
- [18] G. Reyes, J. Comput. Mater. 42 (16) (2008) 1659–1670.
- [19] A.G. Mamalis, K.N. Spentzas, N.G. Pantelelis, D.E. Manolacos, M.B. Ioannidis, Comp. Struct. 83 (2008) 335–340.
- [20] B.A. Gama, T.A. Bogetti, B.K. Fink, C.-J. Yu, T.D. Claar, H.H. Eifert, J.W. Gillespie Jr., Comp. Struct. 52 (2001) 381–395.
- [21] J.A. Reglero, M.A. Rodríguez-Pérez, E. Solórzano, J.A. de Saja, Mater. Des. 32 (2011) 907–910.
- [22] M.F. Ashby, A.G. Evans, N.A. Fleck, L.J. Gibson, J.W. Hutchinson, H.N.G. Wadley, Metal Foams: A Design Guide, Butterworth-Heinemann, Woburn, 2000.
- [23] K. Mohan, Y.T. Hon, S. Idapalapati, H.P. Seow, Mat. Sci. Eng. A 409 (2005) 292–301.
- [24] K. Mohan, PhD thesis, Nanyang Technological University, Singapore, 2007.
- [25] K. Mohan, T.H. Yip, I. Sridhar, Cellular Metals for Structural and Functional Applications Cellmet, Dresden, Germany, 18–20th May 2005, 2005.
- [26] K. Mohan, T.H. Yip, I. Sridhar, J. Mater. Sci. 42 (2007) 3714.